sustainability

MDPI

Article

Investigation of Impact on Hydro-Mechanical Properties for Cement Stabilized Heavy Metal Contaminated Soil under Different Salinity

Xingzhong Nong [1], Yuehua Liang [1], Shan Lin [1], Yi Lu [2] and Zhi Shang [3,*]

[1] Guangzhou Metro Design & Research Institute Co., Ltd., Guangzhou 510010, China
[2] School of Civil Engineering, Guangzhou University, Guangzhou 510006, China
[3] Civil Engineering Discipline, La Trobe University, Melbourne, VIC 3086, Australia
* Correspondence: z2shang@students.latrobe.edu.au

Abstract: The purpose of this study is to investigate the hydro-mechanical properties of heavy metal (Cu, Zn) contaminated soil stabilized using cement treatment situated under different salinity. Conventional oedometers with cylindrical samples dimensioned ∅61.8 × 20 mm were used to conduct the tests. Two cement contents (10%, 20% by mass of cement to the mass of dry soil) and three salinity levels (0.5M, 1M, 1.5M) were used as comparison variables. The compression results demonstrate that the coupled condition in terms of mechanical and chemical will have different behavior on the soil specimen, as Cc (compression index) changes with different metal fractions. The hydraulic conductivity (k) results show that a higher metal fraction will compromise the k. The possible development of water and metal ions is proposed that when a different type and fraction of metal ions are present, the hydration reaction can be suppressed depending on whether the metal ion prioritizes the reaction with either cement or saline solution. It was found that Cu ions prioritize their reaction to a saline solution while Zn ions target the $Ca(OH)_2$ that is available from cement. However, more studies should be carried out to confirm this point.

Keywords: contaminated soil; stabilization/solidification; cement; compressibility; salinity

check for updates

Citation: Nong, X.; Liang, Y.; Lin, S.; Lu, Y.; Shang, Z. Investigation of Impact on Hydro-Mechanical Properties for Cement Stabilized Heavy Metal Contaminated Soil under Different Salinity. *Sustainability* **2022**, *14*, 13901. https://doi.org/10.3390/su142113901

Academic Editors: Pengjiao Jia, Peixin Shi, Xi Jiang and Cheng Cheng

Received: 10 October 2022
Accepted: 24 October 2022
Published: 26 October 2022

Publisher's Note: MDPI stays neutral with regard to jurisdictional claims in published maps and institutional affiliations.

Copyright: © 2022 by the authors. Licensee MDPI, Basel, Switzerland. This article is an open access article distributed under the terms and conditions of the Creative Commons Attribution (CC BY) license (https://creativecommons.org/licenses/by/4.0/).

1. Introduction

As the industry has rapidly developed, the emissions in terms of gas, paints, toxic liquid, etc., have caused a significant impact on the living environment [1]. As the result, heavy metals such as copper (Cu), zinc (Zn), etc can be found in the soil and groundwater [2–7]. These heavy metals are highly plausibly to eventually enter the communities, threatening humans [8,9]. Therefore, controlling the movement of heavy metal to an acceptable level is important for the community. Among the methods for mitigation of heavy metals to the environment, stabilisation/solidification (i.e., S/S) is one cost-effective method to apply [10–14]. The principle of this method is to introduce a binder to prevent heavy metals in the contaminated soils after a series of chemical reactions [15–19]. The most widely used binder is cement, which will result in precipitation formed in the soils [1,20].

The variables such as temperature, pH, and chemical attack have been extensively studied on the mechanical behaviour of heavy metals contaminated soil stabilized with cement [2,5,8,11,19–22]. These studies highlight the mechanism of heavy metal migration in contaminated soil. However, in some coastal cities, the salinity levels in groundwater are higher than the inland cities [23–25]. This will cause the soil not only contain heavy metals but also be exposed to a saline environment [6]. Consequently, a more complicated coupled condition (i.e., heavy metals coupled salinity) is formed to react with cement. In fact, some studies have shown that the low salinity level will help the hydration of cement, so the performance of cemented soil will be enhanced in the later stage [26–28]. Some other

results have shown that the effectiveness of cemented soil in water will be compromised by heavy metals [3,20,29].

It needs to be emphasized that the coupled condition in terms of cement hydration in the saline environment and affected by heavy metals is lacking in the literature. Therefore, the aim of this study is to preliminarily assess the hydro-mechanical performance of heavy metal contaminated soils stabilized by cement in different salinity levels (i.e., NaCl solution).

2. Test Program

2.1. Materials

The kaolin clay (powder form, white color) is supplied by the company of BASF. The specific gravity (G_s) of kaolin clay is given as 2.58. The chemical composition of kaolin in Table 1 is given by the company. The liquid and plastic limit for kaolin is 74% and 32% [30]. The particle size distribution of kaolin shown in Figure 1 is based on the laser diffraction method.

Table 1. Main chemical composition of kaolin is given by BASF.

Composition of Kaolin	Weight%
SiO_2	45.2
Al_2O_3	38.8
NaO_2	0.05–0.3
TiO_2	0.6–1.7
CaO	0.02

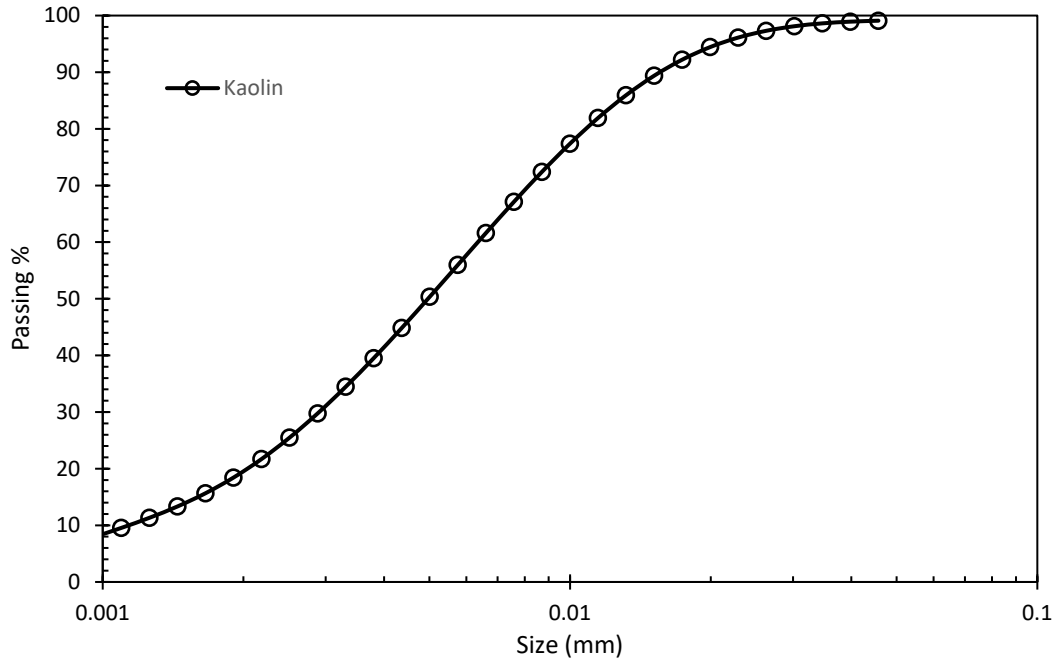


Figure 1. Particle size distribution (PSD) for kaolin clay.

The ordinary Portland cement (OPC) was used as the binder in this study. The G_s of the cement is 3.15. The major chemical composition of the cement includes Calcium Oxide (49%), Silica Oxide (26%), and Aluminum Oxide (11%). Zinc and copper were chosen as the key heavy metals in this study, as they are commonly available metals in contaminated soils. Additionally, the influence of Zinc is more significant than the other commonly available heavy metals [3,20], so the result in this study is expected to have a good contrast. Based

on this feature, the product of Zn (i.e., $Zn(NO_3)_2 \cdot 6H_2O$, Zinc Nitrate Hexahydrate, powder form) and Cu (i.e., $Cu(NO_3)_2 \cdot 3H_2O$, Copper Nitrate Hexahydrate, powder form) were selected. A powder form of NaCl with a purity of over 90% was selected to prepare the saline solution.

2.2. Specimen Preparation

A conventional mixing technique by a laboratory mixer was used for the specimen preparation process [3,20,31]. The ambient temperature of this study was maintained at 20 °C ± 1 °C. A solution with particular concentration of salinity (i.e., 0M, 0.5M and 1M) and heavy metal (i.e., 0M, 0.01M, 0.03M, 0.06M and 0.13M) was prepared in a beaker. The selection of this concentration range of heavy metal is equivalent to 0‰, 0.5‰, 1.5‰, 3‰ and 6‰ in terms of dry soil mass basis for soil after adding to the target water content (Table 2), which falls into the general levels of soil contamination [3,32–34].

Table 2. Summary of experimental conditions.

Soil type	Kaolin
Metal type	Cu, Zn
Cement fraction (%)	10, 20
Salinity (M)	0, 0.5, 1
Metal fraction (‰)	0, 0.5, 1.5, 3, 6
Curing day	14, 28

The kaolin's water content in this study was aimed at approximately 70% which is close to its liquid limit. This will allow the kaolin mix to achieve better workability. This water content is a combination of water and NaCl. After 5 min mixing to reach a slurry consistency, the target cement content (i.e., 10%, 20% on dry soil mass basis) was added to the kaolin and mixed at 120 RPM and 15 min for a good degree of homogeneous state [3]. Afterward, a certain amount of cemented soil bulk was wrapped with vinyl foam and stored in a controlled environment (i.e., 95% in humidity and 20 °C ± 1 °C) to gain some initial strength after 2 days. Subsequently, the cemented soil in the bulk was trimmed into the odometer ring (i.e., 61.8 mm in diameter and 20 mm in height) to form a specimen and wrapped up with the vinyl foam. The wrapped cemented soil specimen in the odometer ring was then returned to the controlled environment for the remaining curing days in this study (i.e., the target curing day was 14 and 28 days). The remaining material from the bulk reserve was also wrapped up and cured in an identical environment to eventually measure the initial condition of each specimen (e.g., water content, density).

After the target curing day was reached, each specimen in the oedometer ring was saturated by a vacuum pump at 100 kPa for 24 h before the tests were conducted [3].

2.3. Test Procedures

When the curing process was finished, the specimen in the oedometer was carefully setup. The corresponding salinity level was then poured into the chamber to provide a consistent salinity environment (i.e., 0M, 0.5M, and 1M). The compressibility test was conducted based on the conventional consolidation test [35,36]. Each loading cycle was terminated by the stabilization of vertical settlement after 24 h. When the whole loading test was finished, the un-loading behavior was also performed to assess the reversibility. The detailed process is demonstrated in Figure 2. The testing environment was controlled at 20 °C ± 1 °C.

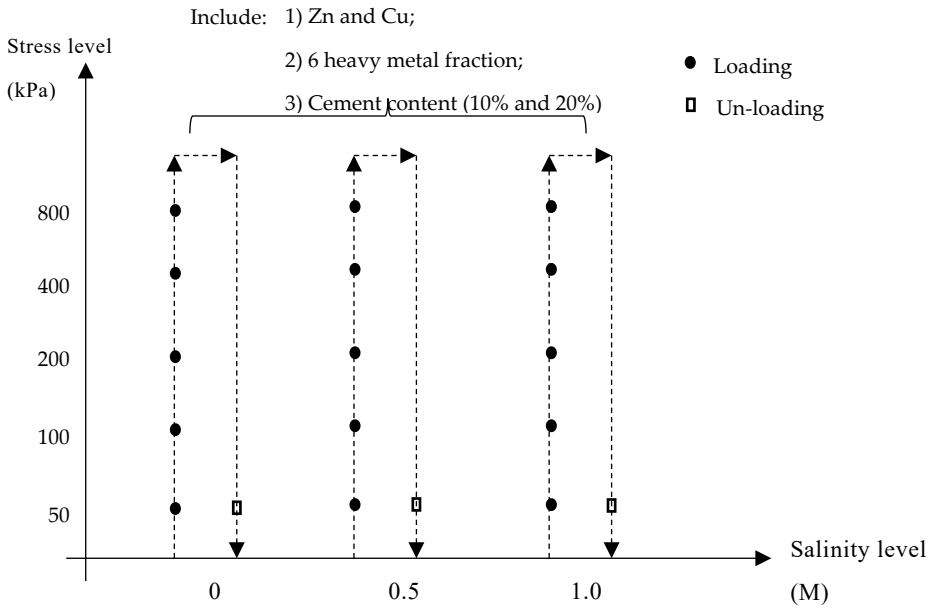


Figure 2. Experimental conditions and procedure.

2.4. Test Procedures

The physical parameter, e (void ratio), is used to describe the relationship between void and solid state in soil. When the value of e is large, more void exists in the soil. Eventually, the soil is more likely to be compressed. The mathematical form to calculate the e is given in Equations (1)–(3).

$$e = \frac{V_v}{V_s} \tag{1}$$

$$V_s = \frac{m_s}{G_s} \tag{2}$$

$$V_v = V - V_s \tag{3}$$

where e is void ratio; V_v is volume of void (cm^3); V_s is volume of solid (cm^3); V is total volume of soil (cm^3); m_s is a mass of solid in a soil (g); G_s is the specific gravity of soil (i.e., 2.58 for kaolin, 2.62 for kaolin and 10% cement, 2.66 for kaolin and 20% cement in this study).

3. Results and Discussions

3.1. Dry Density

Figure 3 demonstrates the variations of dry density after curing in different conditions. It can be seen that the average dry density keeps a horizontal line as the metal fraction increases. This indicates the higher metal fraction in this study has a negligible effect on the dry density. Overall, the average dry density moves upwards at higher concentrations of NaCl solution for both Cu and Zn contaminated soils. At different curing days (i.e., 14 and 28 days), the average dry density for Cu decreases from 1.12 to 1.10 at 1M NaCl solution, 1.10 to 1.06 in 0.5M NaCl solution and 1.05 to 1.03 in 0M NaCl solution (Figure 3a,c). However, at the same condition and curing day, the average dry density remains the same for Zn, which is 1.14 at 1M NaCl solution, 1.11 at 0.5M NaCl solution, and 1.07~1.08 at 0M NaCl solution (Figure 3b,d). Moreover, the average dry density of Zn contaminated soils is slightly higher than Cu-contaminated soils. The comparisons were also made for different cement content for Cu (Figure 3c,e) and Zn (Figure 3d,f). In general, the 20% cement content is about 0.05 to 0.06 higher than 10% cement content in 0M, 0.5M and 1M of NaCl solution.

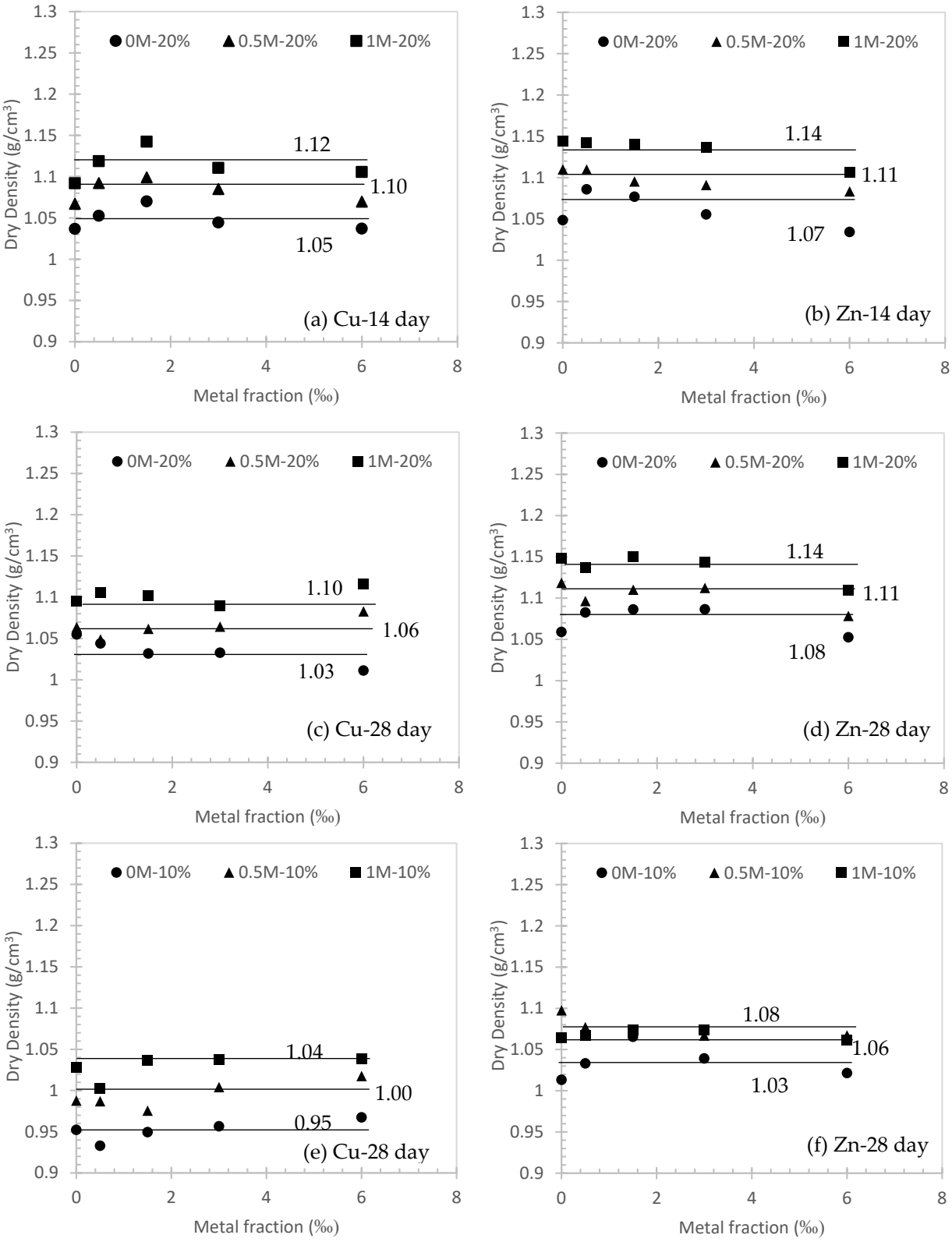


Figure 3. Dry density variation after curing in different conditions.

3.2. Compression Index (Cc) and Swelling Index (Cs)

Figure 4 shows the general compression behavior of specimens under different salinity levels after 14 and 28 days of curing as an example. Accordingly, Cc and Cs were introduced for each condition (Figures 5 and 6).

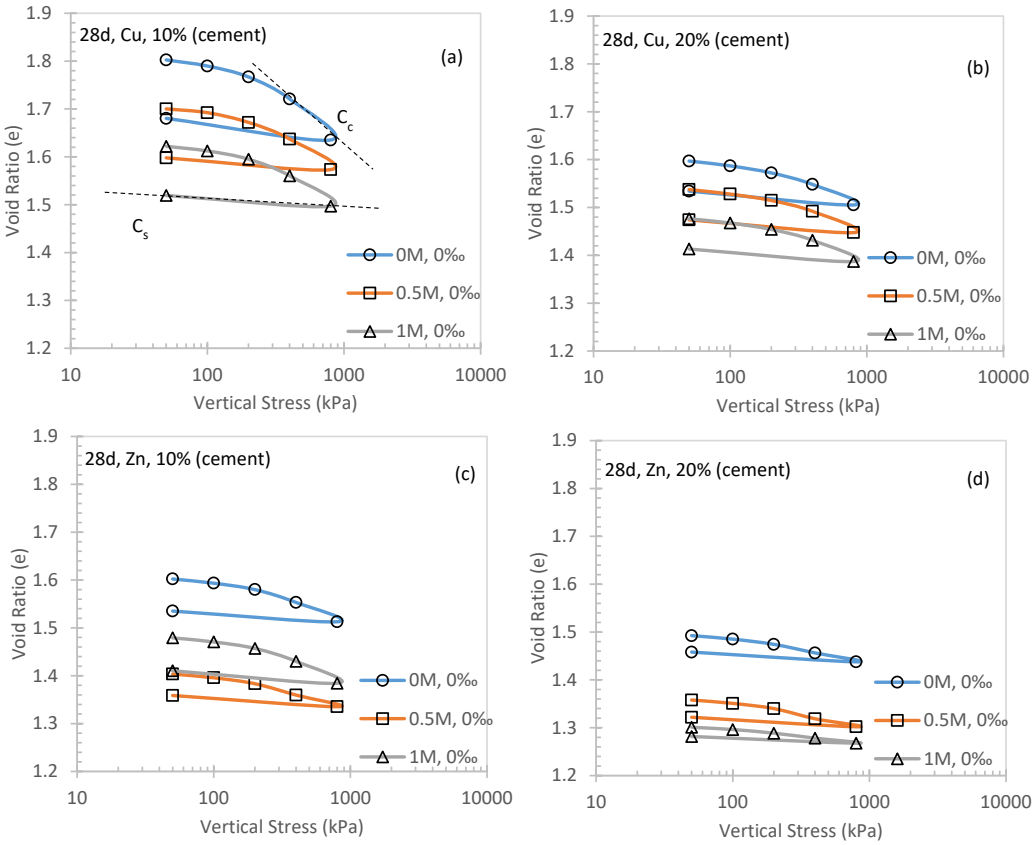


Figure 4. General compression behavior of cemented kaolin clay at 28 days curing for Cu and Zn.

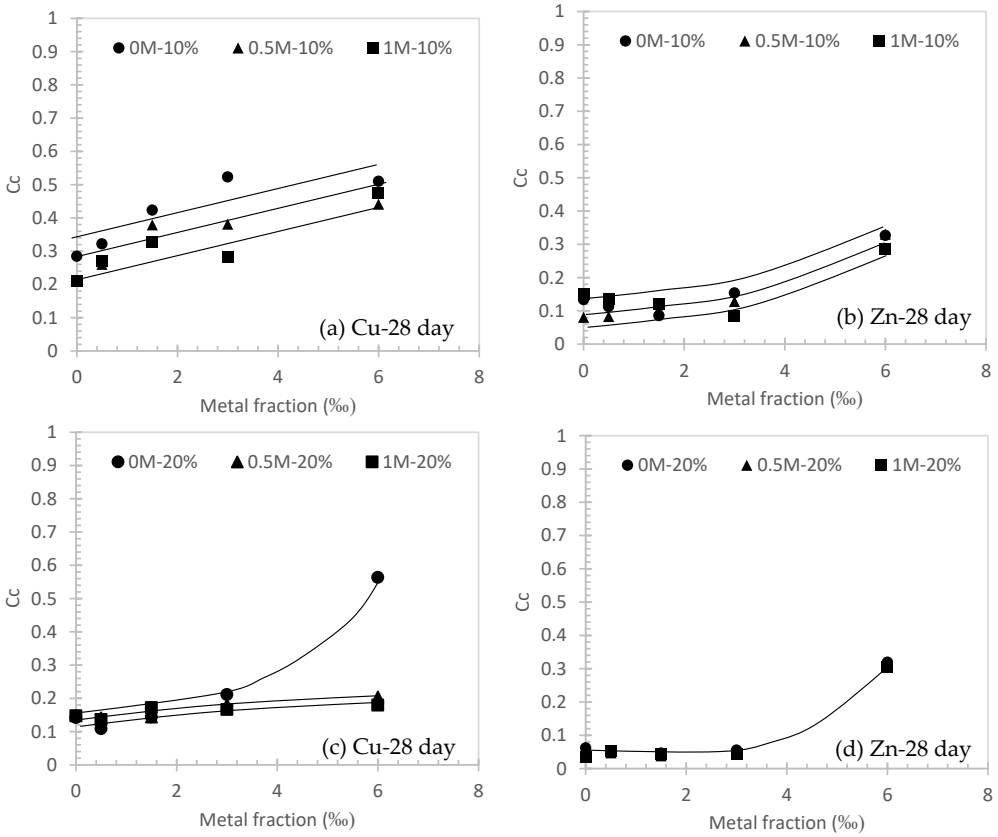


Figure 5. *Cont.*

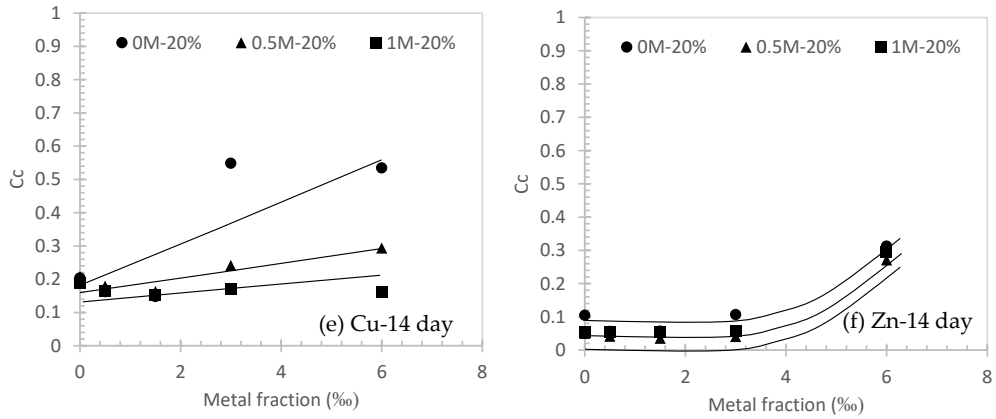


Figure 5. Compression indices (Cc) against metal fraction (‰) in different conditions.

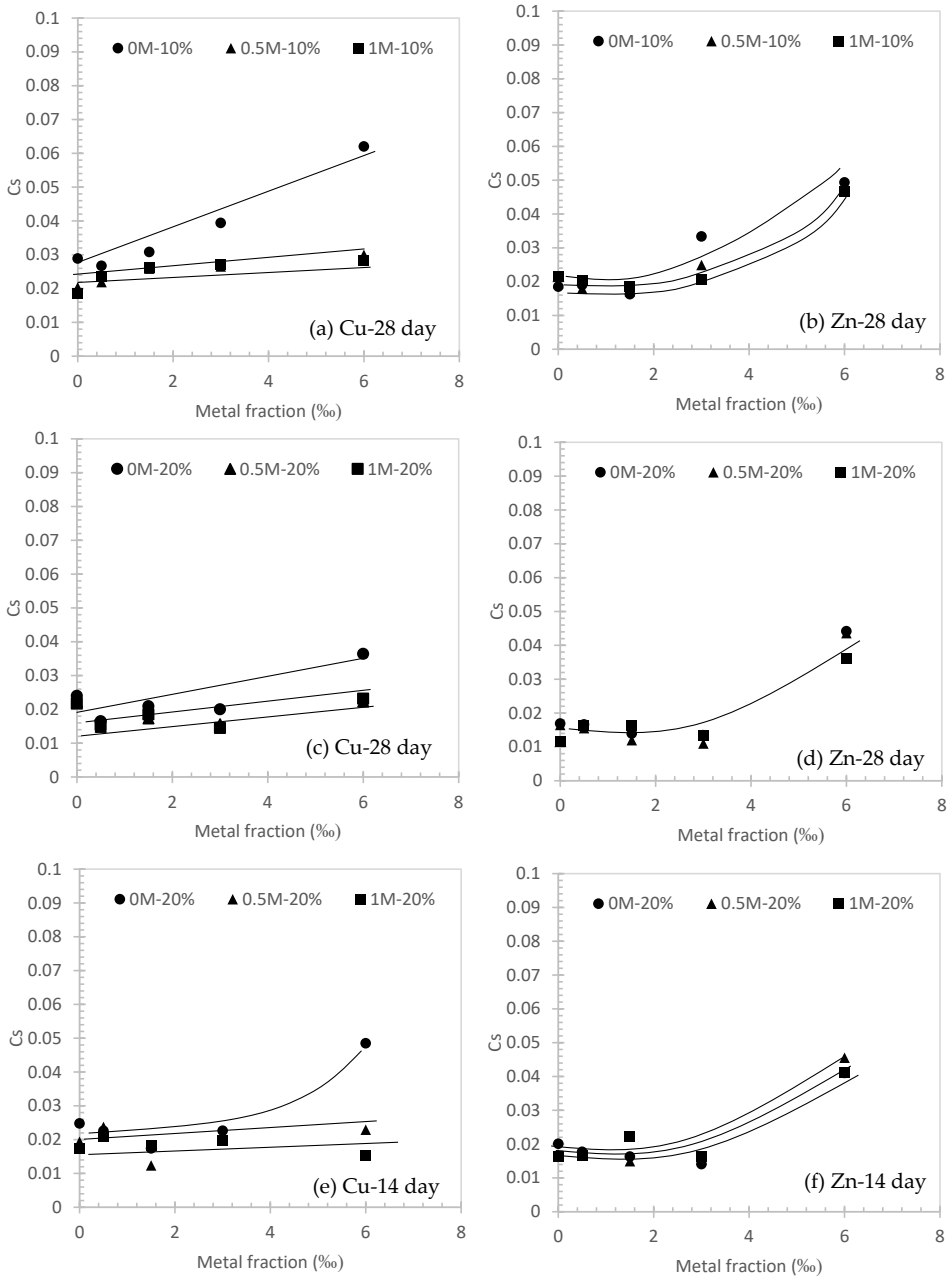


Figure 6. Swelling indices (Cs) against metal fraction (‰) in different conditions.

It can be observed from Figures 4–6 that Cc is always larger than Cs, which is consistent with the elastoplastic theory for conventional soils [37,38]. In Figure 5a,c,e, a positive correlation between Cc and Cu fraction was observed. This suggests that the higher metal fraction in the contaminated soil will induce a stronger compressibility. Significant evidence can be found in Figure 5a (i.e., 28 days curing for 10% cement) and Figure 5e (14 days curing for 20% cement) in three different concentrations of NaCl solution. Additionally, the Cc of 0M Cu specimen is always higher than the 1M counterpart. This can be concluded that the higher concentration of NaCl solution will help to decrease the compressibility of cemented soils (e.g., Figure 5a). It can be also highlighted from Figure 5c that Cc can be compromised by a higher fraction (i.e., Cu at 6‰ in 0M NaCl solution) and decreased to Cc = 0.16 at 6‰ in 0.5M NaCl solution. Similar observations can be made for Zn contaminated soils (Figure 5b,d,f). However, for Figure 5d, the longer curing time (i.e., 28 days) of Zn is observed to have a similar performance to Cc regardless of the salinity levels.

Although higher NaCl concentration will help to enhance the compressibility of cemented soil as mentioned previously, its efficacy was affected by the type of contaminant metal. In Figure 5c, the Cc of 1M NaCl solution Cu specimen is observed to increase from ~0.1 to ~0.16 (about 1.6 times larger) for Cu fraction increases from 0 to 6 ‰, compared with Cc increases from ~0.06 to ~0.32 (about 5 times larger) at the same Zn fraction range (Figure 5d). This evidence shows that Zn compared with other types of heavy metals will significantly compromise the effectiveness of cementation in terms of compressibility, which has been reported by other studies [20]. Figure 5d also implies that there is a turning point of metal fraction, as Cc increases significantly at the Zn fraction beyond 3‰. The cementation is significantly compromised.

Similar behavior for Cs can also be observed in Figure 6. The range of Cs in this study is from 0.06 to 0.01, which can be considered negligible compared to other conventional soils which are usually over 0.1 in Cs [39].

3.3. Hydraulic Conductivity (k)

Terzaghi's one-dimensional compression test can calculate the k of soil (Equation (4)), which is an indirect method to describe the relationship between k and e.

$$k = C_v m_v \gamma_w \tag{4}$$

where C_v is the coefficient of consolidation (m^2/s); m_v is one-dimensional compressibility (kPa^{-1}); k is hydraulic conductivity (m/s); γ_w is the unit weight of water

Figures 7 and 8 show the correlation between k and e at different salinity levels. It can be observed that the cemented soils' k increases when there are more metal fractions and there are no distinctive changes observed from the 0–1.5‰ stage. This can be observed via the SEM photo in Figure 9 that the flocculated Calcium Silicate Hydrate (CSH) has encased the kaolin particles (Figure 9a). The k of 10% cement specimen only increased to 8.69×10^{-9} m/s from 6.67×10^{-9} m/s and an increase from 4.47×10^{-9} m/s to 5.66×10^{-9} m/s at 20% specimen which is insignificant (Figure 7a). A notable change for the 10% cement specimen occurs when the metal fraction was raised from 3‰ to 6‰ (Figure 7c,d). Comparing to the increase to 1.15×10^{-8} m/s from 6.67×10^{-9} m/s observed at 0–1.5‰ the increase in this phase has spiked to 8.56×10^{-8} m/s from 1.6×10^{-8} m/s. The possible reason behind such a phenomenon is that during the process of cement solidification, the gel-formed CSH from cement's hydration reaction will gradually fill the void between soil particles and will decrease the k of the solidified contaminated soil (Figure 10). However, the Cu ion in the specimen will affect the hydration reaction, causing the CSH percentage to rapidly decrease due to increased Cu fraction, resulting in higher e and k (Figure 11a).

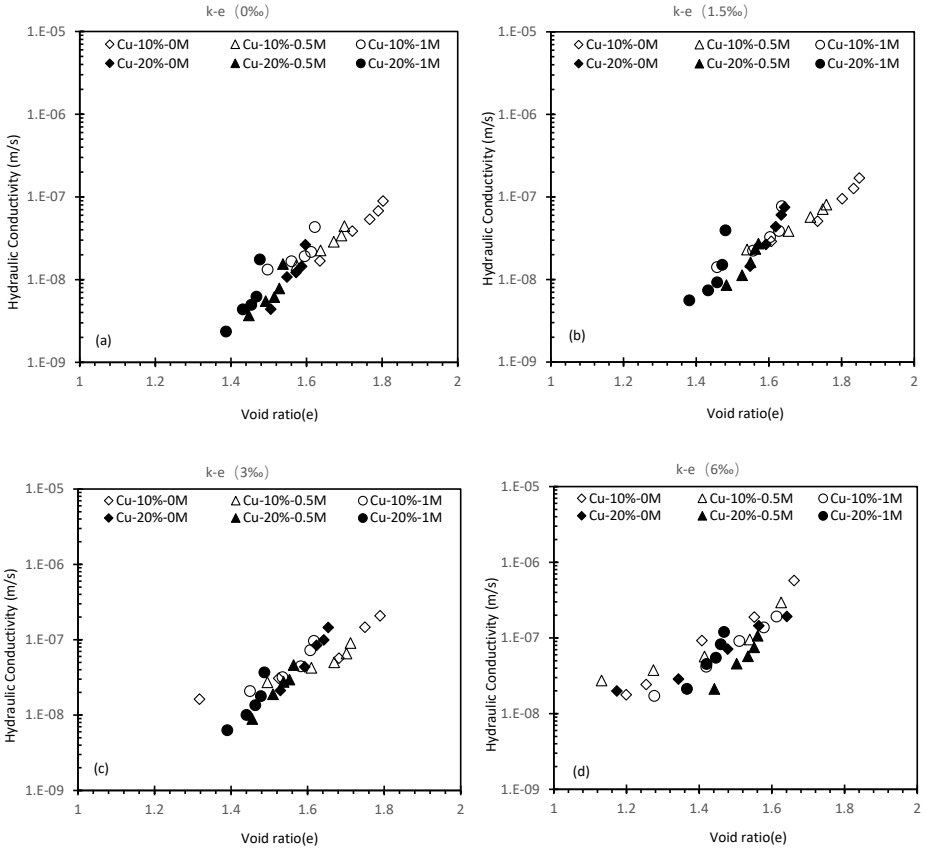


Figure 7. Hydraulic conductivity against a void ratio of 10% and 20% cement Cu specimen.

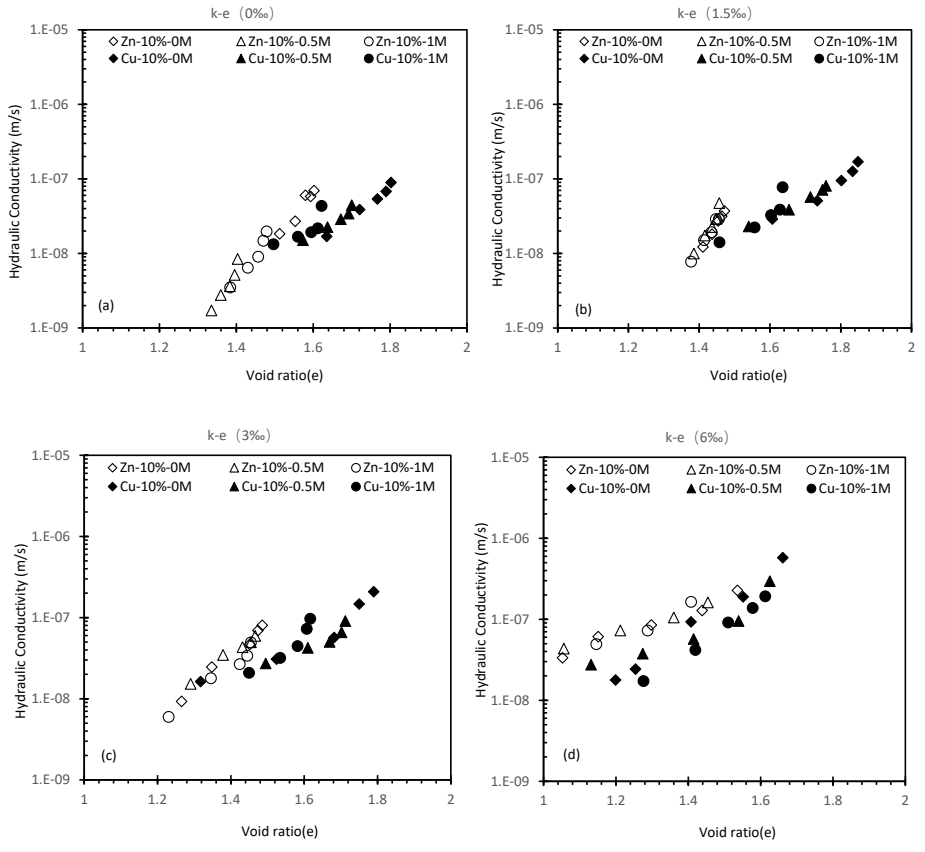


Figure 8. Hydraulic conductivity against a void ratio of 10% cement Zn/Cu specimen.

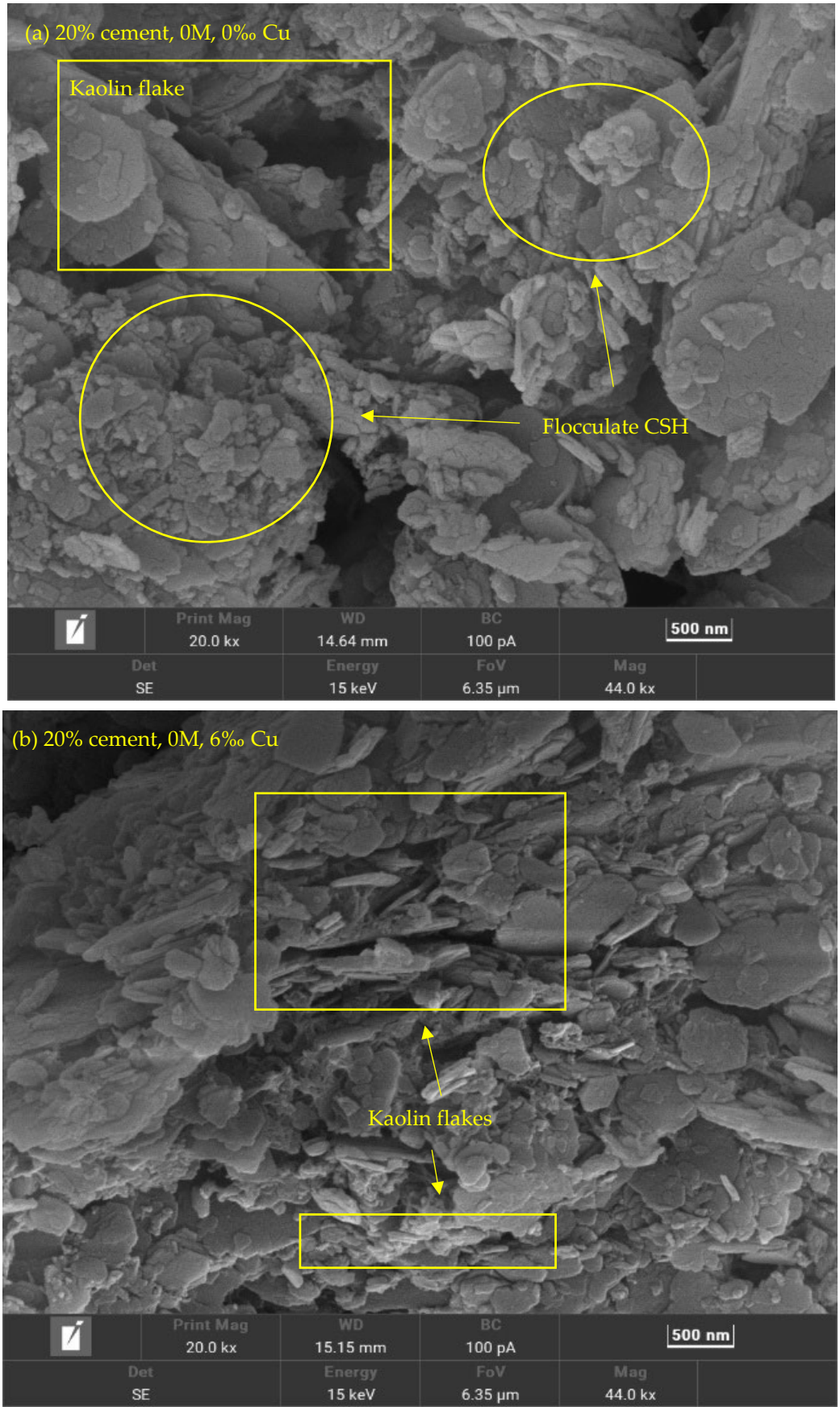
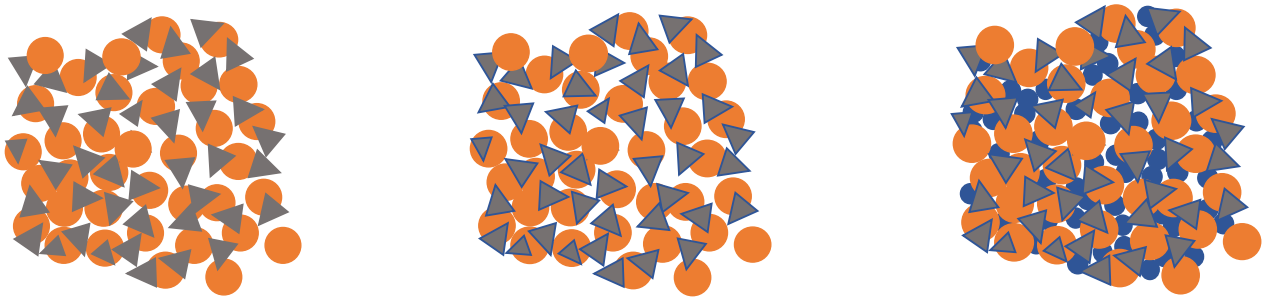


Figure 9. SEM photo of Cu contaminated specimen.

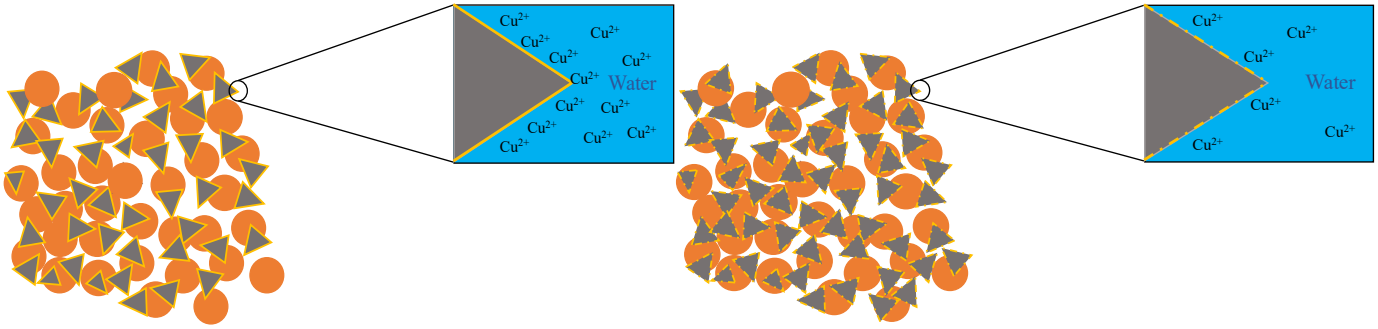


(a) Before reaction, cement particles and soil were uniformly distributed in the soil.

(b) Initial stage of the reaction, CSH gel from hydration reaction forms on the surface of the cement particles

(c) Late stage of the reaction, surface of the soil particle is no longer to hold any more CSH gel, eventually filling the void between soil particles

Figure 10. (**a**) Conceptual drawings of CSH filling the void of soil, including before the reaction, (**b**) early stage of the hydration reaction where CSH forms at the surface of cement particles, and (**c**) eventually filling the void between soil particles.



(a) (b)

Figure 11. (**a**) Conceptual drawing of Cu ion affecting hydration reaction (**b**) and specimen with higher cement content.

It should be worth noting that cement can compromise the k of soil. When the metal fraction is zero, a k reduction from 8.69×10^{-9} m/s to 5.66×10^{-9} m/s can be observed when the cement content was raised to 20%. The efficacy of reduction becomes greater as the metal fraction increases. It is likely that the $Cu(OH)_2$ created from the reaction between OH^- due to hydration reaction and Cu ion have encased the cement particles, suppressing further hydration reaction [40,41]. However, the additional cement particles can relatively compromise the suppression effect. When the hydration reaction continues, more CSH will fill the void, leading to a declined k (Figure 11b). The additional cement did not significantly reduce the k, only a reduction to 5.64×10^{-8} m/s from 8.56×10^{-8} m/s can be seen between 10% and 20% specimen at 6‰ which is negligible since similar changes can be seen at lower concentrations. Therefore, it can be concluded that the hydration reaction of 20% Cu cement content is fully suppressed as the k is similar to the 10% Cu specimen. Figure 8 shows a comparison between the Cu specimen and the Zn specimen under 10% cement content, the result from the Zn specimen shows that the k of Zn specimens is more susceptible to an increased metal fraction.

Results of 10% cement Cu (Figure 7) show that the impact of salinity was not noticeable between 0–1.5‰ metal fraction. A k changed to 2.58×10^{-8} m/s from 1.6×10^{-8} m/s can be found at 3‰ fraction when salinity was increased to 0.5M. Further increasing of salinity yields less improvement. However, in Figure 7 when the salinity was increased to 1M from

0.5M, the *k* increase is significantly higher than 0 to 0.5M. A possible explanation is the amount of cement in the 20% specimen was sufficient to overcome the suppression due to the ion-saline reaction

Similar to the 10% Cu specimen, altering salinity does not significantly change the *k* but the *k* of the Zn specimen under the same metal fraction is always higher than the Cu specimen, which ranges from 6.03×10^{-8} m/s to 8.82×10^{-8} m/s. This can be explained by the compromised compressibility of soil imposed by chlorate salt since chlorate salt can infiltrate the solidification matrix. The NaCl in the saline solution reacts with $Ca(OH)_2$, producing NaOH and $CaCl_2$. Then, $CaCl_2$ will increase the pore volume due to its solubility. Between the NaCl-Cu reaction and NaCl-$Ca(OH)_2$ reaction, the latter is more dominant in terms of quantity and activeness, but the suppression efficiency of this reaction is somewhat inferior to the effect from increasing metal fraction, resulting in more CSH produced at higher salinity. Thus leading to the observation that the *k* decreases at 6‰ despite the increased salinity [40,42]. In the Zn specimens' case, the order of the chemical reaction is the opposite. Zn ions are more active when reacting with $Ca(OH)_2$ than NaCl, therefore the amount of CSH in the Zn specimen is reduced, resulting in a k increase [43–45].

4. Conclusions

This study assesses the hydro-mechanical behavior of Zn- and Cu-contaminated soil stabilized with cement and coupling the saline environment. The corresponding physical parameters in terms of metal fraction, cement content, salinity level, and curing time were investigated. The results obtained from the study suggest that the dry density of cemented specimen was affected by salinity level and a metal fraction has little effect on dry density. An increased metal fraction can elevate the compressibility of soil specimens, while the increase in the salinity will compromise compressibility. The hydraulic conductivity results show that both types of metal will suppress the effect of cementation, resulting in an increase in *k*. The possible reason is that the chemical reaction disrupted the cement hydration reaction. As the CSH from the hydration reaction begins filling the void. Ions from the metal solution can prevent the hydration reaction from continuing. The suppression can be weakened by either increasing cement content or increasing salinity to allow metal ions to prioritize a reaction with NaCl. However, the latter approach only works on certain metals. However, this conclusion suggests more studies should be conducted to confirm this point.

Author Contributions: Conceptualization, Y.L. (Yi Lu) and Z.S.; Data curation, X.N., Y.L. (Yi Lu), and Z.S.; Formal analysis, X.N. and S.L.; Investigation, X.N., Y.L. (Yuehua Liang), S.L. and Z.S.; Methodology, Y.L. (Yuehua Liang); Project administration, Y.L. (Yuehua Liang); Resources, X.N. and Y.L. (Yi Lu); Writing—original draft, S.L., Y.L. (Yi Lu) and Z.S.; Writing—review & editing, Y.L. (Yuehua Liang). All authors have read and agreed to the published version of the manuscript.

Funding: This research was funded by the Ministry of Housing and Urban Rural Development (No. 2022-K-044).

Institutional Review Board Statement: Not applicable.

Informed Consent Statement: Not applicable.

Data Availability Statement: The data used in this study are available upon request.

Conflicts of Interest: The authors declare no conflict of interest.

References

1. Spence, R.D.; Shi, C. *Stabilization and Solidification of Hazardous, Radioactive, and Mixed Wastes*; CRC Press: Boca Raton, FL, USA, 2004; ISBN 0-429-14840-2.
2. Cao, Y.; Guo, L.; Chen, B.; Wu, J. Effect of pre-introduced sodium chloride on cement hydration process. *Adv. Cem. Res.* **2021**, *33*, 526–539. [CrossRef]
3. Du, Y.-J.; Wei, M.-L.; Reddy, K.R.; Jin, F. Compressibility of cement-stabilized zinc-contaminated high plasticity clay. *Nat. Hazards* **2014**, *73*, 671–683. [CrossRef]

4. Du, Y.-J.; Wei, M.-L.; Jin, F.; Liu, Z.-B. Stress–strain relation and strength characteristics of cement treated zinc-contaminated clay. *Eng. Geol.* **2013**, *167*, 20–26. [CrossRef]
5. Liu, J.; Zha, F.; Deng, Y.; Cui, K.; Zhang, X. Effect of an alkaline environment on the engineering behavior of cement-stabilized/solidified Zn-contaminated soils. *Environ. Sci. Pollut. Res.* **2017**, *24*, 28248–28257. [CrossRef] [PubMed]
6. Lu, Y.; Abuel-Naga, H.; Leong, E.-C.; Jiao, W.-G.; Wang, X. Characterisation of geomembrane and geotextile interface short-term creep behaviour in a dry condition. *Geotext. Geomembranes* **2021**. [CrossRef]
7. Li, W.; Yi, Y.; Puppala, A.J. Triaxial strength behavior of carbide sludge (CS)–ground-granulated blastfurnace slag (GGBS)-treated clay slurry. *Acta Geotech.* **2022**. [CrossRef]
8. Shen, Z.; Hou, D.; Zhao, B.; Xu, W.; Ok, Y.S.; Bolan, N.S.; Alessi, D.S. Stability of heavy metals in soil washing residue with and without biochar addition under accelerated ageing. *Sci. Total Environ.* **2018**, *619–620*, 185–193. [CrossRef]
9. Wuana, R.A.; Okieimen, F.E. Heavy Metals in Contaminated Soils: A Review of Sources, Chemistry, Risks and Best Available Strategies for Remediation. *ISRN Ecol.* **2011**, *2011*, 402647. [CrossRef]
10. Cao, X.; Wahbi, A.; Ma, L.; Li, B.; Yang, Y. Immobilization of Zn, Cu, and Pb in contaminated soils using phosphate rock and phosphoric acid. *J. Hazard. Mater.* **2009**, *164*, 555–564. [CrossRef]
11. Gil-Díaz, M.; Alonso, J.; Rodríguez-Valdés, E.; Gallego, J.; Lobo, M. Comparing different commercial zero valent iron nanoparticles to immobilize As and Hg in brownfield soil. *Sci. Total Environ.* **2017**, *584–585*, 1324–1332. [CrossRef]
12. Hale, B.; Evans, L.; Lambert, R. Effects of cement or lime on Cd, Co, Cu, Ni, Pb, Sb and Zn mobility in field-contaminated and aged soils. *J. Hazard. Mater.* **2012**, *199–200*, 119–127. [CrossRef]
13. Harbottle, M.; Al-Tabbaa, A.; Evans, C. A comparison of the technical sustainability of in situ stabilisation/solidification with disposal to landfill. *J. Hazard. Mater.* **2007**, *141*, 430–440. [CrossRef]
14. Lu, Y.; Abuel-Naga, H.; Shaia, H.A.; Shang, Z. Preliminary Study on the Behaviour of Fibre-Reinforced Polymer Piles in Sandy Soils. *Buildings* **2022**, *12*, 1144. [CrossRef]
15. Brown, S.; Christensen, B.; Lombi, E.; McLaughlin, M.; McGrath, S.; Colpaert, J.; Vangronsveld, J. An inter-laboratory study to test the ability of amendments to reduce the availability of Cd, Pb, and Zn in situ. *Environ. Pollut.* **2005**, *138*, 34–45. [CrossRef]
16. Kogbara, R.B.; Al-Tabbaa, A.; Yi, Y.; Stegemann, J.A. Cement–fly ash stabilisation/solidification of contaminated soil: Performance properties and initiation of operating envelopes. *Appl. Geochem.* **2013**, *33*, 64–75. [CrossRef]
17. Kogbara, R.B.; Al-Tabbaa, A.; Yi, Y.; Stegemann, J.A. PH-Dependent Leaching Behaviour and Other Performance Properties of Cement-Treated Mixed Contaminated Soil. *J. Environ. Sci.* **2012**, *24*, 1630–1638. [CrossRef]
18. Kogbara, R.B.; Yi, Y.; Al-Tabbaa, A. Process envelopes for stabilisation/solidification of contaminated soil using lime–slag blend. *Environ. Sci. Pollut. Res.* **2011**, *18*, 1286–1296. [CrossRef]
19. Wang, F.; Shen, Z.; Al-Tabbaa, A. PC-Based and MgO-Based Binders Stabilised/Solidified Heavy Metal-Contaminated Model Soil: Strength and Heavy Metal Speciation in Early Stage. *Géotechnique* **2018**, *68*, 1025–1030. [CrossRef]
20. Li, W.; Ni, P.; Yi, Y. Comparison of reactive magnesia, quick lime, and ordinary Portland cement for stabilization/solidification of heavy metal-contaminated soils. *Sci. Total Environ.* **2019**, *671*, 741–753. [CrossRef]
21. Du, Y.-J.; Jiang, N.-J.; Liu, S.-Y.; Jin, F.; Singh, D.; Puppala, A.J. Engineering properties and microstructural characteristics of cement-stabilized zinc-contaminated kaolin. *Can. Geotech. J.* **2014**, *51*, 289–302. [CrossRef]
22. Liu, J.; Zha, F.; Xu, L.; Kang, B.; Yang, C.; Zhang, W.; Zhang, J.; Liu, Z. Zinc leachability in contaminated soil stabilized/solidified by cement-soda residue under freeze-thaw cycles. *Appl. Clay Sci.* **2020**, *186*, 105474. [CrossRef]
23. Lu, Y.; Abuel-Naga, H.; Leong, E.-C. Mechanical and osmotic consolidation of geosynthetic clay liners: A laboratory study. *Geosynth. Int.* **2020**, *27*, 561–569. [CrossRef]
24. Lu, Y.; Abuel-Naga, H.; Leong, E.-C.; Bouazza, A.; Lock, P. Effect of water salinity on the water retention curve of geosynthetic clay liners. *Geotext. Geomembranes* **2018**, *46*, 707–714. [CrossRef]
25. Lu, Y.; Abuel-Naga, H.; Bouazza, A. Water retention curve of GCLs using a modified sample holder in a chilled-mirror dew-point device. *Geotext. Geomembranes* **2017**, *45*, 23–28. [CrossRef]
26. Pang, X.; Boul, P.; Jimenez, W.C. Isothermal calorimetry study of the effect of chloride accelerators on the hydration kinetics of oil well cement. *Constr. Build. Mater.* **2015**, *77*, 260–269. [CrossRef]
27. Shi, X.; Xie, N.; Fortune, K.; Gong, J. Durability of steel reinforced concrete in chloride environments: An overview. *Constr. Build. Mater.* **2012**, *30*, 125–138. [CrossRef]
28. Shi, Z.; Shi, C.; Liu, H.; Li, P. Effects of triisopropanol amine, sodium chloride and limestone on the compressive strength and hydration of Portland cement. *Constr. Build. Mater.* **2016**, *125*, 210–218. [CrossRef]
29. Li, W.; Yi, Y.; Puppala, A.J. Effects of curing environment and period on performance of lime-GGBS-treated gypseous soil. *Transp. Geotech.* **2022**, *37*, 100848. [CrossRef]
30. *ASTM D4318*; Test Methods for Liquid Limit, Plastic Limit, and Plasticity Index of Soils. ASTM International: West Conshohocken, PA, USA, 2010.
31. AL Rashid, Q.; Abuel-Naga, H.; Leong, E.-C.; Lu, Y.; Abadi, A. Experimental-artificial intelligence approach for characterizing electrical resistivity of partially saturated clay liners. *Appl. Clay Sci.* **2018**, *156*, 1–10. [CrossRef]
32. Chen, L.; Du, Y.-J.; Liu, S.-Y.; Jin, F. Evaluation of Cement Hydration Properties of Cement-Stabilized Lead-Contaminated Soils Using Electrical Resistivity Measurement. *J. Hazard. Toxic Radioact. Waste* **2011**, *15*, 312–320. [CrossRef]

33. Liao, X.-Y.; Chong, Z.-Y.; Yan, X.-L.; Zhao, D. Urban industrial contaminated sites: A new issue in the field of environmental remediation in China. *Huan Jing Ke Xue Huanjing Kexue* **2011**, *32*, 784–794.
34. Voglar, G.E.; Leštan, D. Solidification/stabilisation of metals contaminated industrial soil from former Zn smelter in Celje, Slovenia, using cement as a hydraulic binder. *J. Hazard. Mater.* **2010**, *178*, 926–933. [CrossRef]
35. *ASTM D2435*; Standard Test Method for One-Dimensional Consolidation Properties of Soils. ASTM International: West Conshohocken, PA, USA, 1996.
36. *ASTM D4186*; Standard Test Method for One-Dimensional Consolidation Properties of Saturated Cohesive Soils Using Controlled-Strain Loading. ASTM International: West Conshohocken, PA, USA, 2012.
37. Benessalah, I.; Arab, A.; Sadek, M.; Bouferra, R. Laboratory study on the compressibility of sand–rubber mixtures under one dimensional consolidation loading conditions. *Granul. Matter* **2018**, *21*, 7. [CrossRef]
38. Kodikara, J.; Rahman, F. Effects of specimen consolidation on the laboratory hydraulic conductivity measurement. *Can. Geotech. J.* **2002**, *39*, 908–923. [CrossRef]
39. Tiwari, B.; Ajmera, B. Consolidation and swelling behavior of major clay minerals and their mixtures. *Appl. Clay Sci.* **2011**, *54*, 264–273. [CrossRef]
40. Ray, S.; Mishra, A.K.; Kalamdhad, A.S. Adsorption and Hydraulic Conductivity Studies on Bentonite in Presence of Copper Solution. *J. Hazard. Toxic Radioact. Waste* **2021**, *25*, 06020007. [CrossRef]
41. Tashiro, C.; Oba, J. The effects of Cr2O3, Cu(OH)2, ZnO and PbO on the compressive strength and the hydrates of the hardened C3A paste. *Cem. Concr. Res.* **1979**, *9*, 253–258. [CrossRef]
42. Dutta, J.; Mishra, A.K. Influence of the presence of heavy metals on the behaviour of bentonites. *Environ. Earth Sci.* **2016**, *75*, 993. [CrossRef]
43. Al Khazaaly, S.; Beilby, M.J. Zinc ions block H+/OH− channels in Chara australis. *Plant Cell Environ.* **2012**, *35*, 1380–1392. [CrossRef]
44. Nartowska, E.; Kozłowski, T.; Gawdzik, J. Assessment of the influence of copper and zinc on the microstructural parameters and hydraulic conductivity of bentonites on the basis of SEM tests. *Heliyon* **2019**, *5*, e02142. [CrossRef]
45. Ray, S.; Mishra, A.K.; Kalamdhad, A.S. Adsorption and Hydraulic Conductivity Studies on Bentonites in the Presence of Zinc. In *Advances in Computer Methods and Geomechanics*; Prashant, A., Sachan, A., Desai, C.S., Eds.; Lecture Notes in Civil Engineering; Springer: Singapore, 2020; Volume 55, pp. 489–500. ISBN 9789811508851.